Synthesis, Characterization, Fluorescence and Antibacterial Activity of the Re(VII) Complex $[ReO_3(phen)(H_2PO_4)]\cdot H_2O$

Ahlem Maalaoui[a], Olfa B. Said[b,c], Samah T. Akriche[a], Salem S. Al-Deyab[d], and Mohamed Rzaigui[a]

[a] Laboratoire de Chimie des Matériaux, Faculté des Sciences, 7021 Zarzouna, Bizerte, Tunisie
[b] Equipe Environnement et Microbiologie, IPREM UMR 5254, IBEAS, Université de Pau et des Pays de l'Adour, Pau Cedex, France
[c] Laboratoire de Bactériologie – Pathologie, Institut National des Sciences et Technologies de la Mer (INSTM), Salammbô, Tunisia
[d] Petrochemical Research Chair, College of Science, King Saud University, Riyadh, Saudi Arabia

Reprint requests to M. Rzaigui. E-mail: mohamed.rzaigui@fsb.rnu.tn

Z. Naturforsch. **2012**, *67b*, 1178 – 1184 / DOI: 10.5560/ZNB.2012-0141
Received May 18, 2012

Single crystals of a Re(VII) complex, the dihydrogenophosphato phenanthroline trioxo-rhenium monohydrate of formula $[ReO_3(phen)(H_2PO_4)]\cdot H_2O$ (phen = 1,10-phenanthroline), were prepared in aqueous solution. X-Ray analysis shows that it crystallizes in the monoclinic space group $P2_1/c$ with the unit cell parameters: $a = 8.611(2)$, $b = 13.881(2)$, $c = 14.502(4)$ Å, $\beta = 120.87(2)^\circ$, $V = 1487.9(6)$ Å^3 and $Z = 4$. In the neutral complex, the rhenium is in the oxidation state +VII, coordinated by two nitrogen atoms of the bidentate phen, three terminal oxygen atoms and, for the first time, one oxygen atom of the mono-deprotonated phosphoric acid ligand $H_2PO_4^-$, forming a square-based bipyramidal coordination geometry. The thermal stability, IR, UV/Vis and fluorescence spectroscopic properties are given. The complex shows antimicrobial activity against five different microbes.

Key words: Crystal Structure, Phenanthroline, Rhenium(VII) Complexes, X-Ray Diffraction, Antibacterial Activity

Introduction

The coordination chemistry of Re is actually currently explored intensively owing to use of this element in several fields, more particularly in radiopharmaceuticals for therapy. Rhenium radiopharmaceuticals constitute a class of therapeutic agents in which the bio-distribution is determined by the size, charge and lipophilicity of the complex. Among these compounds, the chemistry of oxo rhenium complexes is of particular interest owing to the favorable nuclear properties of the ^{186}Re and ^{188}Re nuclides, which make the radioisotopes useful for diagnostic nuclear medicine and applications in radioimmunotherapy [1 – 3] and radiopharmaceuticals [4, 5]. Thus, the coordination chemistry of rhenium complexes is well developed, and a variety of complexes containing rhenium in the formal oxydation states +I, +III, +IV, +V, and +VII have been described and characterized [6]. X-Ray investigations have indicated that heptavalent rhenium, in addition to its role in the most important perrhenate ions, is capable of forming more complicated oxo complexes with coordination numbers six and five [7]. While the complexes including the trioxo group (ReO_3) are numerous [6, 8 – 13], the complexes with the principal structural unit $[(phen)ReO_3]$ remain still relatively scarce. The best known representatives are those published elsewhere [6, 7]. In this paper, we report the synthesis of a novel trioxo-rhenium complex, $[ReO_3(phen)(H_2PO_4)]\cdot H_2O$ (**1**), involving for the first time the dihydrogenphosphate anion ($H_2PO_4^-$) as a ligand together with phen. The crystal structure, the thermal behavior, spectroscopic properties, and antibacterial activity are also reported.

Results and Discussion

Complex **1** was synthesized by mixing phen and NH_4ReO_4 in water-ethanol medium followed by the addition of $NaBH_4$ and phosphoric acid.

Crystal and molecular structure

The asymmetric unit of **1** contains one Re(VII) atom surrounded by one chelating phenanthroline, one monodentate $H_2PO_4^-$ ligand, three terminal oxide units, and one water molecule of crystallization (Fig. 1). The neutral $[ReO_3(phen)(H_2PO_4)]\cdot H_2O$ units are linked by different intra- and intermolecular interactions to develop a 3D network (Fig. 2). These interactions are mainly hydrogen bonds of the kind O–H···O ranging from 2.596(9) to 2.890(9) Å and C–H···O between the phenanthroline molecules and the oxygen atoms of the dihydrogenphosphate groups with distances D···A ranging from 3.019(9) to 3.416(8) Å (Table 1). The C–H···O hydrogen bond parameters lie in the typical range observed for these interactions [14].

In the $[ReO_3(phen)(H_2PO_4)]$ entity, the rhenium atom has an distorted octahedral environment of formula ReN_2O_4. The geometrical characteristics of this octahedron show that it is a square-based bipyramid with a basal plane built up of two terminal oxygen atoms (O5 and O6) and two nitrogen atoms (N1 and N2) of a phenanthroline molecule. The four in-plane atoms N1, N2, O5, and O6 are coplanar (r. m. s. deviation = 0.0701 Å). The tetragonality (defined by the mean in-plane bond length divided by the mean out-of-plane bond length) is 1.047 [15]. The Re atom lies 0.16 Å above this plane towards O1. As shown in Table 2, the distances Re–N1 (2.247(5) Å) and Re–N2 (2.249(5) Å) are significantly longer than Re–O5 (1.716(4) Å) and Re–O6 (1.720(4) Å) due to the fact that O5 and O6 are terminal oxygen atoms. The axial coordination sites are occupied by a terminal oxygen atom (O7) and an oxygen atom (O1) of a monodentate dihydrogenphosphate group at distances Re–O1 = 2.097(4) Å and Re–O7 = 1.709(5) Å. The ReN_2O_4 polyhedron shares one of its vertices with a H_2PO_4 tetrahedron. This dihydrogenphosphate group involves O–P–O angles ranging from 100.9(3) to 113.4(4)°. The P–OH bonds, 1.555(6) and 1.556(5) Å, are longer than the coordinated P–O bond (1.518(5) Å), which is longer than the unco-

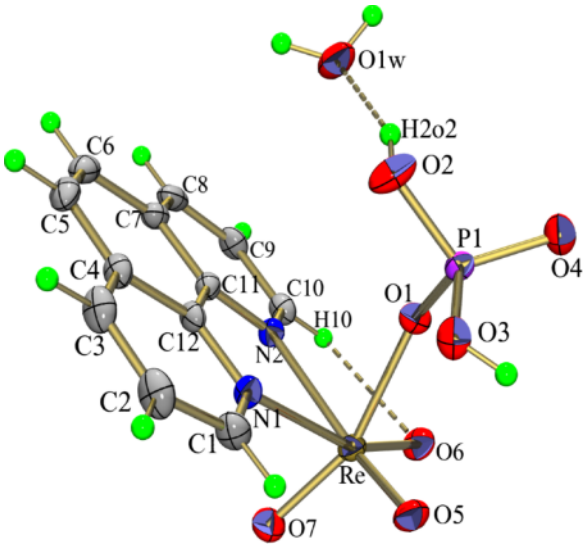

Fig. 1. ORTEP view of $[ReO_3(phen)(H_2PO_4)]\cdot H_2O$ (**1**). Displacement ellipsoids are drawn at the 30 % probability level. H atoms are represented as small spheres of arbitrary radii. Hydrogen bonds are shown as dashed lines.

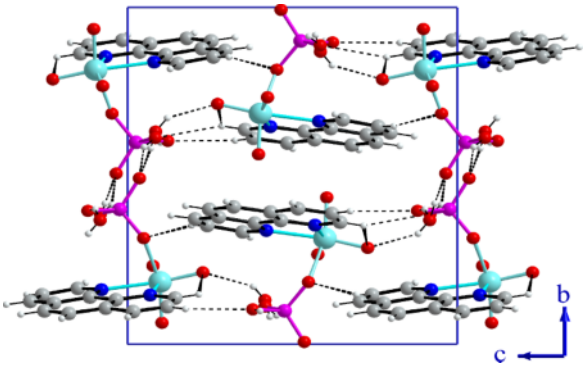

Fig. 2. Projection of the packing of the molecules of **1** along the *a* axis.

Table 1. Main interatomic distances (Å) and angles (deg) involved in the hydrogen bonding scheme of complex **1**[a].

D–H···*A*	*D*–H	H···*A*	*D*···*A*	*D*–H···*A*
O2–H2*O2*···O1W	0.82	1.82	2.596(9)	157
O3–H3*O3*···O4^{i}	0.82	1.85	2.601(7)	151
O1W–H2W1···O4^{ii}	0.85	1.90	2.725(7)	166
O1W–H1W1···O6^{iii}	0.85	2.14	2.890(8)	147
C2–H2···O1^{iv}	0.93	2.48	3.384(9)	165
C9–H9···O2^{v}	0.93	2.56	3.344(10)	143
C10–H10···O6	0.93	2.56	3.019(9)	111
C10–H10···O3^{v}	0.93	2.56	3.416(8)	153

[a] Symmetry codes: (i) $-x+1, -y, -z+1$; (ii) $-x+2, -y, -z+1$; (iii) $x+1, -y+1/2, z+1/2$; (iv) $x, -y+1/2, z+1/2$; (v) $x, -y+1/2, z-1/2$.

Table 2. Selected bond lengths (Å), and angles (deg) for **1** with estimated standard deviations in parentheses.

Distances	
Re–N1	2.247(5)
Re–N2	2.249(5)
Re–O1	2.085(5)
Re–O5	1.711(6)
Re1–O6	1.721(5)
Re1–O7	1.714(6)
Bond angles	
O5–Re–O7	103.0(3)
O6–Re–N1	158.2(2)
O5–Re–O6	106.8(3)
O1–Re–N1	77.7(2)
O7–Re–O6	103.3(3)
O5–Re–O1	89.3(2)
O7–Re–N2	86.7(3)
O7–Re–O1	159.2(3)
O5–Re–N2	159.4(2)
O6–Re–N2	88.2(2)
O6–Re–O1	88.8(2)
O1–Re–N2	76.8(2)
O5–Re–N1	90.2(2)
N1–Re–N2	72.3(2)
O7–Re–N1	85.5(2)

ordinated one (1.482(5) Å). This behavior is consistent with the general observation in numerous phosphates [16]. The shortest intermolecular Re···Re separation is 6.062(2) Å. In the crystal structure, the packing of the molecules appears to be influenced by $\pi\cdots\pi$ stacking interactions between parts of the phenanthroline ring systems of neighboring molecules, with a mean inter-planar distance of 3.358 Å. The distances between the centroids of the C4C5C6C7C11 and N2C10C9C8C7C11 rings and their symmetry-equivalents at $2-x$, $1-y$, $1-z$ are 3.558(3) and 3.5595(1) Å, respectively. The $\pi\cdots\pi$ interactions and the H-bonding lead to the formation of a cohesive three-dimensional network.

IR and UV/Vis properties

The IR spectrum of $[ReO_3(phen)(H_2PO_4)]\cdot H_2O$ (Fig. 3) exhibits characteristic bands of its different components. The terminal Re=O groups are characterized by stretching modes at 1002 and 983 cm^{-1}. The Re–O and Re–N groups linked to ligands have stretching modes between 870 and 725 cm^{-1} [17 – 19]. These modes were identified for other Re(VII) complexes containing chelating ligands in their coordination sphere [20, 21]. The phen-based absorptions

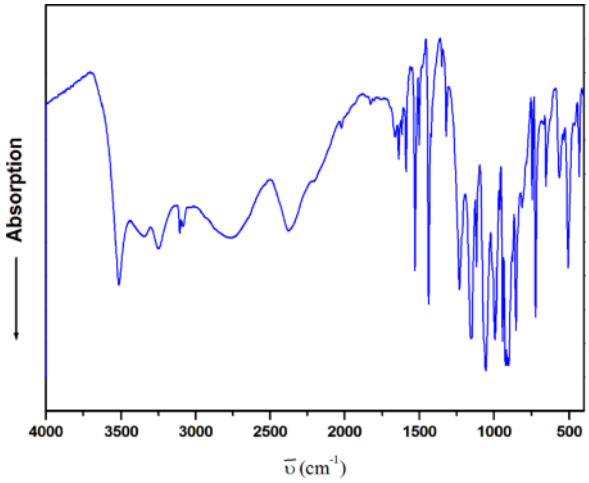

Fig. 3. The room-temperature IR spectrum of $[ReO_3(phen)(H_2PO_4)]\cdot H_2O$ (**1**).

(1619, 1579, 1539, 1507, 844, 733, and 625 cm^{-1}) are characteristic of the chelating form of this ligand. Specific bands of $H_2PO_4^-$ (1017, 938 cm^{-1}) are observed, too [22]. The range 2500 – 3600 cm^{-1} contains several bands, which could be assigned to the stretching modes of the water molecule, the hydroxyl group of the phosphate ligand and the =C-H groups of phenanthroline [23].

The electronic spectrum of **1** in DMSO solution recorded between 260 and 400 nm is shown in Fig. 4b. It shows two significant UV absorption bands with maxima at about 279 and 285 nm. These higher energy absorptions in the 260 – 300 nm region should be assigned to the admixture of ligand-based π–$\pi*$ charge transfer (ILCT/LLCT). These assignments are confirmed by the absorption spectra of free phen (Fig. 4a) and the results for related systems [24, 25]. The energy gap (Fig. 5) between the frontier orbitals [the highest occupied molecular orbital (HOMO) and the lowest unoccupied molecular orbital (LUMO)] was determined using the Tauc model [26] as 4.2 eV. This value is quite large and indicates that **1** is relatively stable in terms of energy and has a high chemical hardness.

Fluorescence properties

The solid-state fluorescence spectrum of **1** at room temperature is depicted in Fig. 6. It exhibits an intense blue fluorescence with an emission maximum at *ca.*

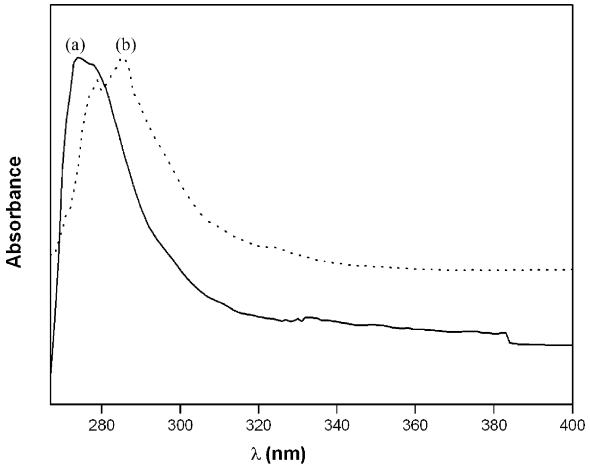

Fig. 4. Absorption spectra of (a) pure phenanthroline and (b) $[ReO_3(phen)(H_2PO_4)]\cdot H_2O$ (**1**).

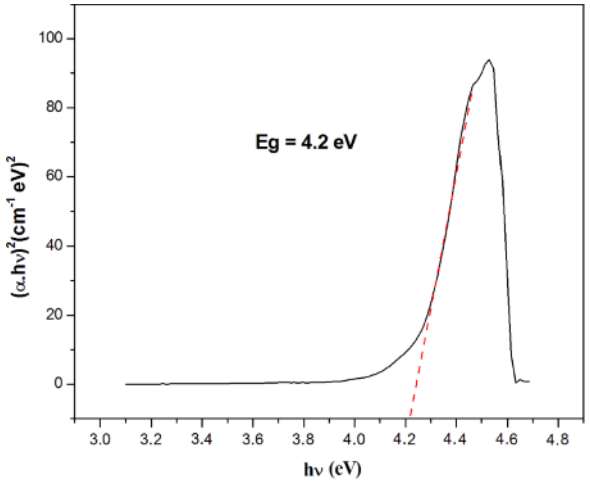

Fig. 5 (color online). Determination of the energy gap for complex **1** according the Tauc model [26].

424 nm and a weak peak at *ca.* 480 nm (Fig. 6c) upon excitation at *ca.* 320 nm. The free 1,10-phenanthroline ligand in the solid state at room temperature presents a similar spectrum built up from a broad band with an emission maximum at *ca.* 365 and a weak peak at *ca.* 400 nm (Fig. 6b) upon excitation at *ca.* 290 nm. Therefore, the emission of **1** may be assigned to intraligand transitions (ILCT). By comparing the emission spectra of **1** and of the ligand we can conclude that the fluorescence enhancement in **1** may be due to both coordination and packing interactions. The fluorescence red-shift of the emission energy on going from the

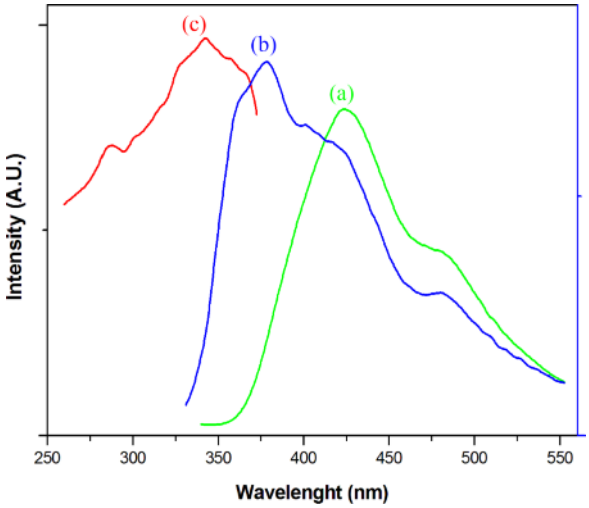

Fig. 6 (color online). Optical spectra of complex **1** and free phenanthroline. (a) Emission spectrum of complex **1** in the solid state; (b) emission spectrum of free phenanthroline in the solid state; (c) excitation spectrum of complex **1** in the solid state.

free ligand to the complex appears to be related to the phen-phen $\pi\cdots\pi$ stacking interactions, which results in a decrease in the HOMO-LUMO energy gap of the complex [27].

Thermal properties

The simultaneous TG-DTA analyses of the title compound were carried out in air. The obtained curves (Fig. 7) show that this compound is thermally stable up to 120 °C and exhibits two main thermal decomposition processes over a wide temperature range (120 – 600 °C). In a first step, $[ReO_3(phen)(H_2PO_4)]\cdot H_2O$ undergoes a dehydration (at *ca.* 158 °C), accompanied with an experimental weight loss of 4 %, very close to that calculated (3.4 %). Above 160 °C the obtained anhydrous phase undergoes, over a wide temperature range, several decomposition phenomena represented by a series of endothermic peaks on the DTA curve and by two successive weight losses. The sum of both weight losses (37 %) corresponds to the organic component (34 %), leaving an unidentified phosphate of rhenium contaminated with fine particles of black carbon. Similar thermal behavior has been observed for other rhenium complexes [28, 29].

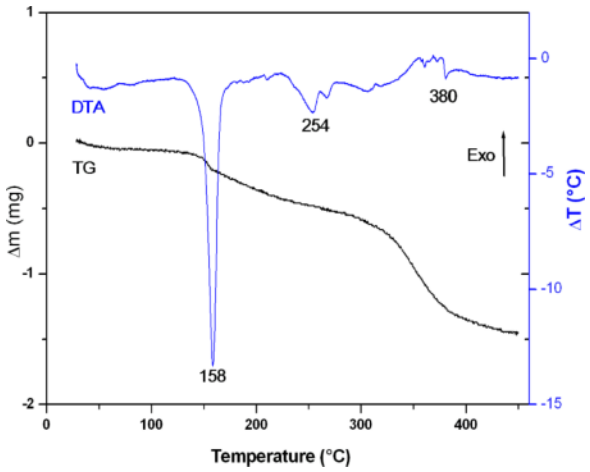

Fig. 7 (color online). DTA and TGA curves of $[ReO_3(phen)(H_2PO_4)]\cdot H_2O$ (**1**), at rising temperature.

Antibacterial activity

The study of the *in vitro* antibacterial activity of complex **1** in DMSO has shown that it has varying degrees of significant inhibition of the tested microorganisms (Fig. 8). The DMSO solvent was completely inactive against the five used bacteria. To our knowledge, antimicrobial activity has been observed previously only in the case of rhenium(V) complexes [30 – 32] which inhibit the multiplication process of the microbes by blocking their active sites [33, 34]. It was reported [35 – 37] that the following five principal factors are relevant: (i) the chelate effect of the ligands, (ii) the nature of the *N*-donor ligands, (iii) the total charge of the complex, (iv) the nature of the counterion, and (v) the nuclearity of the metal center in the complex.

Conclusion

Interaction of perrhenates with phosphoric acid and phenanthroline in aqueous solution leads to the neutral complex **1**. The rhenium atom is in oxidation state (VII) and has a square-based bipyramidal environment of formula ReN_2O_4. A 3D network characterizes the crystal structure where the components develop different intra- and intermolecular interactions (H-bonds, van der Waals contacts, $\pi\cdots\pi$ stacking). This complex, thermally stable up to 120 °C, exhibits intense blue fluorescence around 424 and 480 nm upon excitation at 320 nm. In addition, the *in vitro* antibacterial screening against five mico-organisms reveals that it exhibits a wide spectrum of antibacterial activity. Therefore, this complex could be a promising candidate for applications.

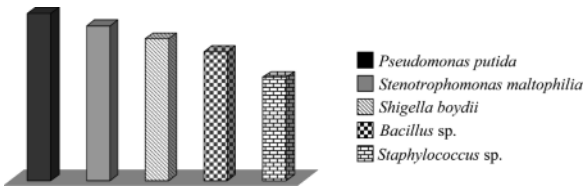

Fig. 8. The inhibition zone of $[ReO_3(phen)(H_2PO_4)]\cdot H_2O$ (**1**) in DMSO on five kinds of bacteria.

Experimental Section

Synthesis

Starting materials were purchased from commercial sources and used without further purification. To a solution of phenantroline (0.18 g, 1 mmol) in ethanol (25 mL), 25 mL of distilled water and 0.27 g (1 mmol) of NH_4ReO_4 were added and the mixture stirred until dissolution. Addition of a pinch of $NaBH_4$ gave an effervescent brown solution with formation of a blackish precipitate. Then, commercial phosphoric acid was added dropwise with stirring until complete dissolution of the precipitate. The obtained solution was subjected to a slow evaporation of the solvent until the formation of brown crystals stable in air at room temperature and suitable for X-ray diffraction. Yield after one week: 36 %. – UV/Vis (DMSO): λ_{max} ($\log\varepsilon$) = 279 (5.03), 285 nm (5.11). – PXR [main lines: *d* (Å)/*hkl*/*I* (%)]: 9.31/011/20; 7.34/100 & $\bar{1}\bar{1}$1/40; 6.94/020/25; 6.51/110/23; 6.19/002/21; 6.07/$\bar{1}$12 & 021/100; 5.68/012/35; 5.42/$\bar{1}\bar{2}$1/15; 5.06/120/29; 4.311/031 & $\bar{2}$02/31; 4.080/$\bar{2}\bar{1}$2 & $\bar{1}\bar{3}$1/41; 3.569/210 & 023/31.

X-Ray crystal structure determination

The powder diffraction pattern was obtained using a D8 Advance Bruker powder diffractometer with Cu K_α ($\lambda = 1.5418$ Å) radiation. A suitable single crystal of **1** for X-ray analysis was mounted on an Enraf-Nonius Mach3 diffractometer equipped with a graphite monochromator using Ag K_α radiation ($\lambda = 0.56087$ Å). Data were collected at 293 K. Crystallographic data and refinement results of complex **1** are given in Table 3. Unit cell parameters were determined from least-squares refinement of 25 reflections. 7273 independent reflections were measured of which 5136 had $I > 2\sigma$ (I) and were used for structure determination and refinement. The structure was solved by Direct Methods using the program SHELXS-97 [38, 39] in the WINGX

Table 3. Crystal data, data collection and structure refinement details for **1**.

Chemical formula	$[ReO_3H_2PO_4(C_{12}H_8N_2)]\cdot H_2O$
Formula weight	529.41
Crystal size, mm^3	$0.50 \times 0.20 \times 0.10$
Crystal system	monoclinic
Space group	$P2_1/c$
a, Å	8.611(2)
b, Å	13.881(2)
c, Å	14.502(4)
β, deg	120.866(17)
V, $Å^3$	1487.9(6)
Z	4
D_{calcd}, $g\,cm^{-3}$	2.36
$\mu(Ag K_\alpha)$, mm^{-1}	4.5
$F(000)$, e	1008
θ range for data collection, deg	2–27.96
Reflections collected	10 040
Independent reflections/R_{int}	7273/0.02
Absorption correction	multi-scan
$T_{min/max}$	0.221/0.469
Refined param./restraints	219/3
Final $R1/wR2$[a,b] $[I > 2\sigma(I)]$	0.050/0.122
Final $R1/wR2$[a,b] (all data)	0.080/0.135
GoF (F^2)[c]	1.05
$\Delta\rho_{max/min}$, e $Å^{-3}$	4.39/ − 3.56

[a] $R1 = \Sigma||F_o| - |F_c||/\Sigma|F_o|$; [b] $wR2 = [\Sigma w(F_o^2 - F_c^2)^2/\Sigma w(F_o^2)^2]^{1/2}$, $w = [\sigma^2(F_o^2) + (AP)^2 + BP]^{-1}$, where $P = (\mathrm{Max}(F_o^2, 0) + 2F_c^2)/3$; [c] $\mathrm{GoF} = [\Sigma w(F_o^2 - F_c^2)^2/(n_{obs} - n_{param})]^{1/2}$.

package [40, 41], and refined on F^2 by full-matrix least-squares methods using the SHELXL-97 program [38, 39]. All non-hydrogen atoms were refined isotropically and then anisotropically. All hydrogen atoms were placed geometrically and treated as riding. The hydrogen bonding scheme and selected bond lengths and angles are given respectively in Tables 1 and 2. The molecular graphics were drawn using ORTEP-3 [42] and DIAMOND [43].

CCDC 872796 contains the supplementary crystallographic data for this paper. These data can be obtained free of charge from The Cambridge Crystallographic Data Centre *via* www.ccdc.cam.ac.uk/data_request/cif.

Thermal analysis

Thermal analysis was performed using a multimodule 92 Setaram analyzer operating from room temperature up to 500 °C at an average heating rate of 5 °C min^{-1}. Experiments were carried out in air with a finely ground sample of 12.3 mg.

Spectroscopic measurements

The IR spectrum was recorded in the range $4000 - 400\,cm^{-1}$ with a Perkin-Elmer Spectrum BXII spectrometer using a sample dispersed in a spectroscopically pure KBr pellet. The UV/Vis spectrum in DMSO was obtained using a Lamda 11 Perkin-Elmer spectrophotometer. Excitation and emission spectra were measured with a Perkin-Elmer LS55 Fluorimeter using solid samples at room temperature.

Antibacterial activity

The antibacterial experiments were performed following the modified methodology published in [44, 45]. Various pathogenic organisms were treated by a 2×10^{-3} M solution (optimal concentration) of complex **1** in DMSO. Five bacterial strains, *Pseudomonas putida* DQ989291, *Stenotrophomonas maltophilia* DQ230920, *Shigella boydii* AY696681, *Staphylococcus* sp. DQ978267, and *Bacillus* sp. EF026993 were grown in Petri dishes. Mueller-Hinton agar plates were loaded with a 4×10^6 CFU mL^{-1} suspension of the strain. Small holes made in the agar were inoculated with 100 μL of sample solutions. After incubation for 24 h at 37 °C, the inhibition halo diameters were measured in mm.

Acknowledgement

The authors express their appreciation to the Tunisian Ministry of Higher Education and Scientific Research and the Deanship of Scientific Research at King Saud University for funding the paper through the Research Group Project no. RGP-VPP-089.

[1] B. Noll, C. S. Hilger, P. Leibnitz, H. Spies, *Radiochim. Acta* **2004**, *92*, 271.
[2] A. Zablotskaya, I. Segal, S. Germane, I. Shestakova, E. Lukevics, T. Kniess, H. Spies, *Appl. Organomet. Chem.* **2002**, *16*, 550.
[3] H. Zhang, M. Dai, C. Qi, B. Li, X. Guo, *Applied Radiation and Isotopes* **2004**, *60*, 643.
[4] W. Volkert, W. F. Goeckeler, G. J. Ehrhardt, A. R. Ketring, *J. Nucl. Med.* **1991**, *32*, 174.
[5] E. A. Deutsch, K. Libson, J. L. Vanderheyden, *Technetium and Rhenium in Chemistry and Nuclear Medicine*, Raven Press, New York **1990**.
[6] H. Braband, S. Imstepf, M. Felber, B. Spingler, R. Alberto, *Inorg. Chem.* **2010**, *49*, 1283.
[7] T. Lis, *Acta Crystallogr.* **1987**, *C43*, 1710.
[8] F. E. Kuhn, J. J. Haider, E. Herdtweck, W. A. Herrmann, A. D. Lopes, M. Pillinger, C. C. Romão, *Inorg. Chim. Acta* **1998**, *279*, 44.

[9] V. S. Sergienko, T. S. Khodashova, M. A. Porai-Koshits, L. A. Butman, *Koord. Khim. (Russ)* **1977**, *3*, 1060.

[10] J. Y. K. Cheng, K. K. Cheung, M. C. W. Chan, K. Y. Wong, C. M. Che, *Inorg. Chim. Acta* **1998**, *272*, 176.

[11] K. Wieghardt, C. Pomp, B. Nuber, J. Weiss, *Inorg. Chem.* **1986**, *25*, 1659.

[12] W. A. Herrmann, P. W. Roesky, F. E. Kuhn, W. Scherer, M. Kleine, *Angew. Chem., Int. Ed.* **1993**, *32*, 1714.

[13] W. A. Herrmann, P. W. Roesky, F. E. Kuhn, M. Ellison, G. Artus, W. Scherer, C. C. Romão, A. Lopes, J. M. Basset, *Inorg. Chem.* **1995**, *34*, 4701.

[14] G. R. Desiraju, *Crystal Engineering: The Design of Organic Solids*, Elsevier, New York **1989**.

[15] A. W. Addison, T. N. Rao, J. Reedijk, J. Van Rijn, G. C. Verschoor, *J. Chem. Soc., Dalton Trans.* **1984**, 1349.

[16] H. Hebert, *Acta Crystallogr.* **1978**, *B34*, 611.

[17] J. Mink, G. Kresztury, A. Stirling, W. A. Herrmann, *Spectrochim. Acta* **1994**, *A50*, 2039.

[18] P. G. Edwards, J. Jokela, A. Lehtonen, R. Sillanpää, *J. Chem. Soc*., *Dalton Trans.* **1998**, 3287.

[19] F. A. Cotton, G. Wilkinson, C. A. Murillo, M. Bochmann, *Advanced Inorganic Chemistry*, 6th ed., Wiley, New York **1999**.

[20] A. Davison, A. G. Jones, M. J. Abrams, *Inorg. Chem.* **1981**, *20*, 4300.

[21] A. Guest, C. J. L. Lock, *Can. J. Chem.* **1971**, *49*, 603.

[22] K. Nakamoto, *Infrared and Raman Spectra of Inorganic and Coordination Compounds*, 3rd, Wiley-Interscience, New York **1978**.

[23] R. J. H. Clark, C. S. Williams, *Spectrochim. Acta* **1965**, *A21*, 1861.

[24] Z. Si, X. Li, X. Li, H. Zhang, *J. Organomet. Chem.* **2009**, *694*, 3742.

[25] Z. Si, J. Li, B. Li, F. Zhao, S. Liu, W. Li, *Inorg. Chem.* **2007**, *46*, 6155.

[26] J. Tauc, *Mater. Res. Bull.* **1968**, *3*, 37.

[27] H. Yersin, A. Vogler, *Photochemistry and Photophysics of Coordination Compounds*, Springer, Berlin **1987**.

[28] R. Mahfouz, E. Al-Frag, M. R. H. Siddiqui, W. Z. Alkiali, O. Karam, *Arabian J. of Chem.* **2011**, *4*, 119.

[29] P. A. Shcheglov, D. V. Drobot, *Chem. Mater.* **2002**, *14*, 2378.

[30] M. M. Mashal, H. F. El-Shafiy, S. B. El-Maraghy, H. A. Habib, *Spectrochim. Acta* **2005**, *A61*, 1853.

[31] M. M. Mashaly, T. T. Ismail, S. B. El-Maraghy, H. A. Habib, *J. Coord. Chem.* **2003**, *56*, 1307.

[32] M. M. Mashaly, *J. Coord. Chem.* **2003**, *56*, 833.

[33] N. Sari, S. Arslan, E. Logolu, I. Sakiyan, *J. Sci.* **2003**, *16*, 283.

[34] L. Mishra, V. K. Singh, *Indian J. Chem.* **1993**, *A32*, 446.

[35] A. D. Russell in *Disinfection, Sterilization and Preservation*, 4th ed., (Ed.: S. S. Block), Lea and Febinger, Philadelphia **1991**, pp. 27 – 59.

[36] H. W. Rossmore in *Disinfection, Sterilization and Preservation*, 4th ed., (Ed.: S. S. Block), Lea and Febinger, Philadelphia **1991**, pp. 290 – 321.

[37] G. Psomas, A. Tarushi, E. K. Efthimiadou, Y. Sanakis, C. P. Raptopoulou, N. Katsaros, *J. Inorg. Biochem.* **2006**, *100*, 1764.

[38] G. M. Sheldrick, SHELXS/L-97, Programs for Crystal Structure Determination, University of Göttingen, Göttingen (Germany) **1997**.

[39] G. M. Sheldrick, *Acta Crystallogr.* **2008**, *A64*, 112.

[40] L. J. Farrugia, WINGX, A MS-Windows System of Programs for Solving, Refining and Analysing Single Crystal X-ray Diffraction Data for Small Molecules, University of Glasgow, Glasgow, Scotland (UK) **2005**.

[41] L. J. Farrugia, *J. Appl. Crystallogr.* **1999**, *32*, 837.

[42] C. K. Johnson, M. N. Burnett, ORTEP-III (version 1.0.2), Rep. ORNL-6895, Oak Ridge National Laboratory, Oak Ridge, TN (USA) **1996**.

[43] K. Brandenburg, DIAMOND, Crystal and Molecular Structure Visualization, Crystal Impact – K. Brandenburg & H. Putz GbR, Bonn (Germany) **2004**. See also: http://www.crystalimpact.com/diamond/.

[44] C. Reyes, J. Fernandez, J. Freer, M. A. Mondaca, C. Zaror, S. Malato, H. D. Mansilla, *J. Photochem. Photobiol.* **2006**, *A184*, 141.

[45] O. Ben Said, M. S. Goni-Urriza, M. El Bour, M. Dellali, P. Aissa, R. Duran, *J. Appl. Microbiol.* **2008**, *104*, 987.